GESEP – Gerência de Especialistas em Sistemas Elétricos de Potência

Título:

Power Losses in Photovoltaic Inverter Components due to Reactive Power Injection

Autores:

ANDRADE, E. G.; OLIVEIRA, H. A.; RIBEIRO, W. V.; BARROS, R. C.; CUPERTINO, A. F.; PEREIRA, H. A.

Publicado em:

International Conference on Industry Applications (INDUSCON)

Data da publicação:

2016

Citação para a versão publicada:

ANDRADE, E. G. ; OLIVEIRA, H. A. ; RIBEIRO, W. V. ; BARROS, R. C. ; CUPERTINO, A. F. ; PEREIRA, H. A. Power Losses in Photovoltaic Inverter Components due to Reactive Power Injection. In: International Conference on Industry Applications, 2016, Curitiba. INDUSCON, 2016.

Power Losses in Photovoltaic Inverter Components due to Reactive Power Injection

Eduardo G. de Andrade, Hadassa A. de Oliveira, Wesley V. Ribeiro, Rodrigo C. de Barros, Heverton A. Pereira
Gerência de Especialistas em Sistemas Elétricos de Potência
Federal University of Viçosa - UFV
Viçosa, MG, Brazil
eduardogeike@gmail.com, hadassa.14ab@gmail.com, wv.ribeiro92@hotmail.com, rodrigocdebarros@gmail.com, heverton.pereira@ufv.br

Allan F. Cupertino
Departamento de Engenharia de Materiais
Centro Federal de Educação Tecnológica de Minas Gerais
Belo Horizonte, MG, Brazil
allan.cupertino@yahoo.com.br

***Abstract*— The grid power stability is significantly affected as a result of the net impact of many small photovoltaic (PV) generators, since there is an increase of PV systems connected to distribution systems. There are many ways to improve the system stability, regarding voltage regulation. Some work proposes to use the PV inverter idle capacity to support reactive power to the grid. The main drawback of this solution is the increase of losses in the converter during this additional functionality. Therefore, this paper analyzes the power losses in the PV inverter components (IGBTs, diodes, a dc-link capacitor and damping resistance) during both active and reactive power injection. Simulations considering a 5kW three-phase PV inverter are performed with focus in conduction and switching losses, besides, the temperature in the semiconductor devices.**

INTRODUCTION

In the last decades, the interest in solar photovoltaic (PV) energy has increased considerable around the world. According to European Photovoltaic Industry, solar power had a record year in 2014 with 40 GW being connected worldwide which beats the record of the previous year, when 37 GW were connected. Also, PV system price declines of around 75% in less than 10 years have brought solar power close to cost competitiveness in several countries and market segment [1]. However, the growth of renewable energy, especially photovoltaic sources, makes the grid more decentralized and susceptible to disturbances. This fact is bringing some concerns to professionals in these areas and one of the most discussed points is the grid power quality due to use of power electronic based-converters.

Nonetheless, there has been growing interest in the use of multifunctional inverters to improve the ac-grid power quality [2] [3]. Thus, PV inverters usually perform the task of supply active power during the daytime, can ancillary the main grid with reactive power support during nighttime or during low-profile irradiance. [4] However, reliability issues come into picture with this additional utilization. This extra work-time during nights causes additional thermal stress and consequently decreasing the inverter efficiency and lifetime [5].

Power losses on the power electronics devices are inevitable, bringing as direct consequence a heating of these components. Temperature changes of the power devices will affect the reliability, since thermal cycling has been one of the most observed factors that cause failures in power devices [6]. Some components of the PV inverters, such as diodes and IGBTs, are more sensible to thermal effects [7].

From all factors aforementioned, this paper proposes to analyze a 5 kW three-phase PV inverter losses while reactive power injection is added as an ancillary service. The losses estimation is focused on conduction and switching losses in semiconductor switches (IGBTs and diodes). Furthermore, the losses in damping resistor and dc-link capacitor are considered.

This paper is structured as follows: Section II provides the description of a three-phase grid-connected PV inverter and the control strategy implemented to regulate the active and reactive power flow. Also, the main sources of losses in the inverter are presented; those sources include the IGBTs and diodes, the damping resistors from the LCL filter, and the dc-link capacitor. A thermal model of the semiconductors devices including the losses analysis is provided in Section III. The determination of the total power losses of the components at different values of reactive and active power injection are given in Section IV. Conclusions are stated in Section V.

CONTROL STRATEGY

A schematic of a three-phase grid-connected control structure is shown in Fig 1. The case study of this paper considers a three-phase two level inverter with a LCL filter. The solar arrays and the dc/dc stage are modeled by means of a current source connected directly to the dc bus.

This work is supported by the Brazilian agencies CAPES, FAPEMIG and CNPQ.

The control strategy is implemented in synchronous reference frame and it is based in two cascaded loops: inner control loops, controlling the injected direct and quadrature currents, and the outer control loops, controlling the dc bus voltage and the reactive power injected into the grid. Since the control is performed in synchronous-reference frame, a Phase-Locked Loop (PLL) structure is used in order to synchronize the system. The complete control strategy is shown in Fig 2.

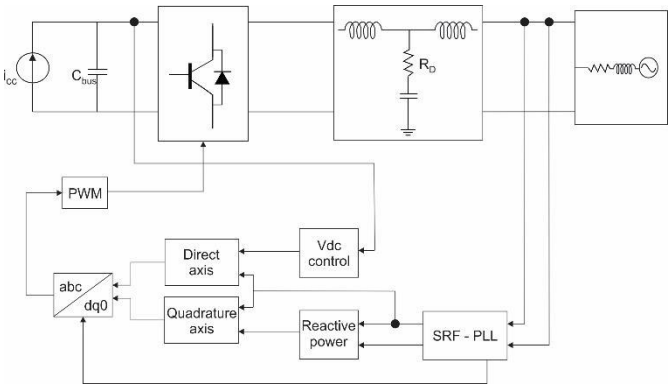

Figure 1 Electric and control diagram of a simplified three-phase PV inverter.

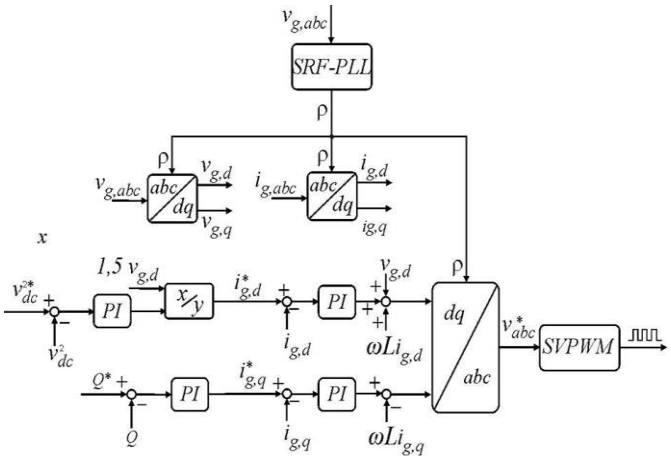

Figure 2. Detailed control schematic.

A) Inner Control Loop

In the used control strategy, the inner loops control the direct and quadrature axis current, and the closed-loop transfer function is given by:

$$\frac{I_{d,q}(s)}{I^*_{d,q}(s)} = \frac{1/R}{L/R\,s+1} k_{i1} \frac{(k_{p1}/k_i s + 1)}{s} \qquad (1)$$

where $R = R_f + R_g$ and $L = L_f + L_g$, from the equivalent simplified circuit of the c.a. side inverter.

Since the PV inverter plants for direct and quadrature current axes are equal, it can be used the same gains for both current loops. Also, the parameters of the controllers were found using the method of poles placement. The inner loop gains are presented in Table I.

B) Outer Control Loop

1) Reactive Power Control

In (2) is described the transfer function of the reactive power loop PI control.

$$\frac{Q(s)}{Q^*(s)} = \frac{1+T_1 s}{1+T_2 s} \qquad (2)$$

where $T_2 = \frac{1+Hk_{p2}}{Hk_{i2}}$,and $T_1 = \frac{k_{p2}}{k_{2i}}$ and $H = -\frac{3}{2}v_g$.

Considering poles placement method, it is possible to define a cut-off frequency and thus the controller gains. All gains used in this work are shown in Table I.

2) DC-Link Voltage Control

The dynamic equation of the square of dc bus voltage is given by:

$$\frac{dv_{dc}^2}{dt} = \frac{2(P_{PV} - P_C)}{C_{dc}} \qquad (3)$$

where $P_{PV}$is the active power generated by solar panels and $P_C$is the active power drawn by the converter.

Applying Laplace transform in (3), the close-loop considering a PI controller is given by:

$$\frac{V_{dc}^2}{V_{dc}^{*2}} = \frac{2(sk_{p,bus} + k_{i,bus})}{Cs^2 + 2(sk_{p,bus} + k_{i,bus})} \qquad (4)$$

Similarly to reactive power control strategy, the inner loop gains are calculated considering pole allocation method, as follows in Table I.

TABLE I. CONTROL PARAMETERS

Parameter	***Value***	***Parameter***	***Value***
V_g	310,27 V	$K_{p,bus}$	0.1131
$K_{p,pll}$	0.5728	$K_{i,bus}$	3.553
$K_{i,pll}$	50.8958	$K_{p,react}$	-6.579 e-4
R_{cbus}	220 mΩ	$K_{i,react}$	-0.2480
L_f	1.5 mH	R_d	0.4 Ω
C_f	8.71 µF	L_g	1.5 mH
C_{bus}	1 mF	L	3 mH

LOSSES CALCULATION AND THERMAL MODEL

C) Loss Calculations to IGBT

The losses in the IGBT can be broken down into the conduction $(P_{S,cond})$ and switching $(P_{S,sw})$ losses. The total losses are giving by

$$P_{S\,Tot} = P_{S,cond} + P_{S,sw}. \qquad (6)$$

Conduction losses occur when the device is in full conduction. The current in the device is required by the circuit and the voltage at its terminals is the voltage drop due to the

device itself. These losses are in direct relationship with the duty cycle (Dc) .

The voltage across the IGBT is the sum of the IGBT ON-state current collector–emitter voltage $(vce0)$ and a multiplication of the collector current (ic) with collector–emitter ON-state resistance (rc):

$$v_{ce}(ic) = v_{ce0} + rc \times ic. \quad (7)$$

The instantaneous value of the IGBT conduction loss is:

$$P_{S.Cond,inst} = v_{ce}(ic) \times ic = v_{ce0} \times ic + rc \times ic^2. \quad (8)$$

Considering that the IGBT conducts for half a period, the value of the $P_{S.Cond}$ can be evaluated by:

$$P_{S.Cond} = \int_0^{\frac{t_{sw}}{2}} (P_{S.Cond,inst} \times Dc)\, dt = v_{ce0} \times i_{c,av} + rc \times ic^2{}_{\text{ms}} \quad (9)$$

where $i_{c,av}$ is the overage collector current and the ic_{ms} is the root mean square (rms) value of the collector current [10].

Switching losses occur when the device is transitioning from the blocking state (Es_{OFF}) to the conducting state (Es_{ON}) and vice-versa. This interval is characterized by a significant voltage across its terminals and a significant current through it. The energy dissipated in each transition needs to be multiplied by the frequency (fsw) in order to obtain the switching losses:

$$P_{S,sw} = (Es_{ON} + Es_{OFF}) \times fsw \quad (10)$$

In this work is used six IGBTs, with part number IKW15N120H3-DS.The thermal model was simulated using the simulation platform for power electronics PLECs. The conduction and switching losses specification are presented in Fig 4 and Fig 5, respectively.

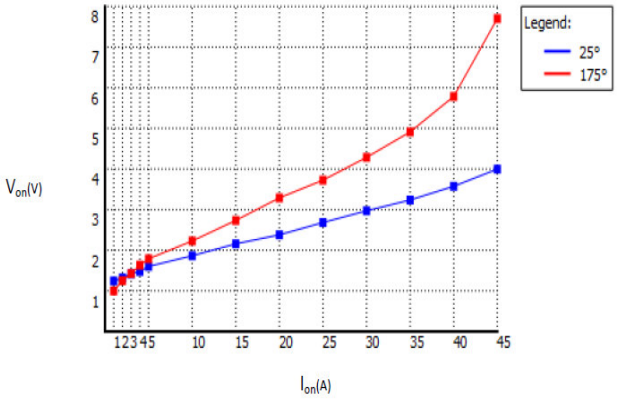

Figure 4. IGBT Thermal Model: Conduction losses.

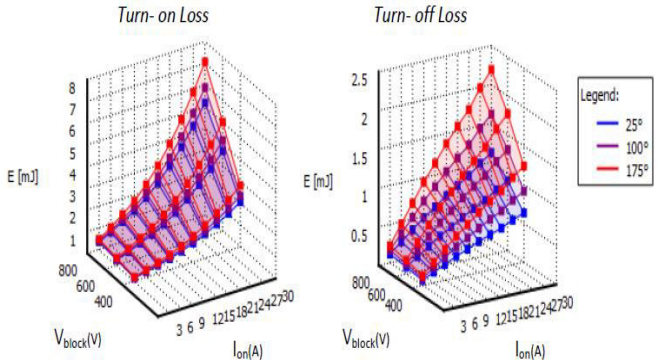

Figure 5. IGBT Thermal Model: Switching losses.

D) *Loss Calculations to Diode*

The loss calculations in a diode are similar to the IGBT method showed in Section III.C. The instantaneous power value of a diode in conduction mode $(P_{D.Cond,inst})$ is given by:

$$P_{D.Cond,inst} = v_d(id) \times id = v_{d0} \times id + rd \times id^2. \quad (11)$$

Where, v_d and id represents the voltage and the current over the diode, respectively. Also, v_{d0} is the ON-state voltage across the diode and rd is the diode ON-state resistance. Integrating over a period of (1- Dc, the period where the diode conducts, the $P_{D.Cond}$ is giving by (12):

$$P_{D.Cond} = \int_0^{\frac{t_{sw}}{2}} (P_{D.Cond,inst} \times (1 - Dc))\, dt = v_{d0} \times i_{d,av} + rd \times id^2{}_{ms} \quad (52)$$

where $i_{d,av}$ is the average diode current and id_{ms} is the rms value of the diode current.

To calculate the diode switching losses, the turn-on energy is usually assumed to be zero [11]. Also, the turn-off energy (Es, OFF) is estimated from the reverse recovery energy loss during a small period. Therefore, the Ps, sw can be found by multiplying the Es_{OFF} by the frequency.

$$P_{S,sw} = (Es_{OFF}) \times \text{fsw} \quad (13)$$

The thermal model was build using the same method for the IGBT. The diode part number used in this work is IKW15N120H3-DS. Using its specification, a thermal model was generated on PLECS simulator. The thermal parameters are showed in Fig 6 and Fig 7.

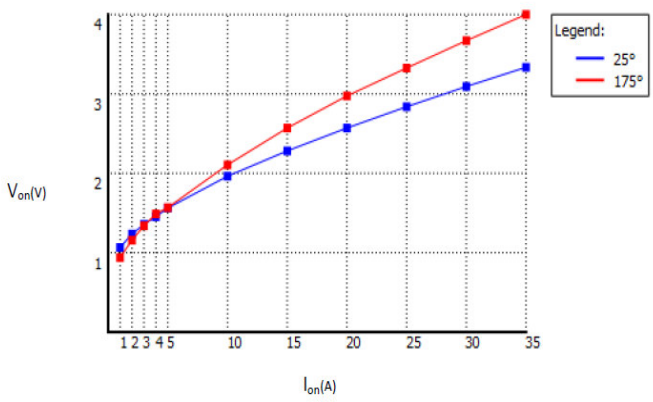

Figure 6. Diode Thermal Model: Conduction losses.

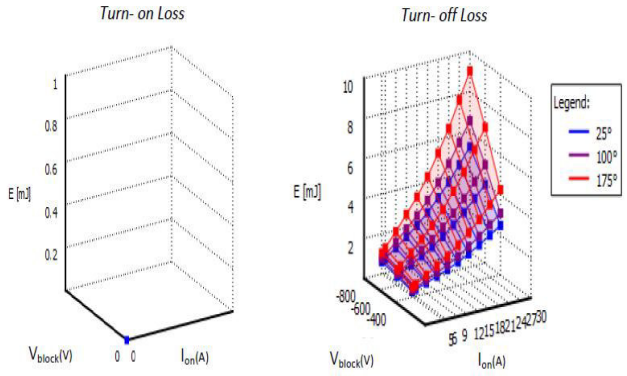

Figure 7: Diode Thermal Model: switching losses.

E) Aditional Losses

Besides the most significant losses (from IGBTs and diodes), the PV inverter presents other significant losses on the ac-filter damping resistors and the internal resistor from the dc-bus capacitance, respectively, R_d and R_{cbus}. Their losses are calculated through the resistor power given by:

$$P_R = Ri^2 \quad (14)$$

SIMULATION AND RESULTS

The simulation was made using a 5kW three-phase inverter, and it was broken into three different simulations. In the first simulation, the active power (P) was gradually increased from 1kW to its maximum (5kW) while the reactive power (Q) was kept unchanged. In the second simulation, the reactive power was increased while the active power was kept unchanged. Finally, in the third simulation the active and reactive power were applied together. The injected grid power can be seen in Fig.8 and Fig.9.

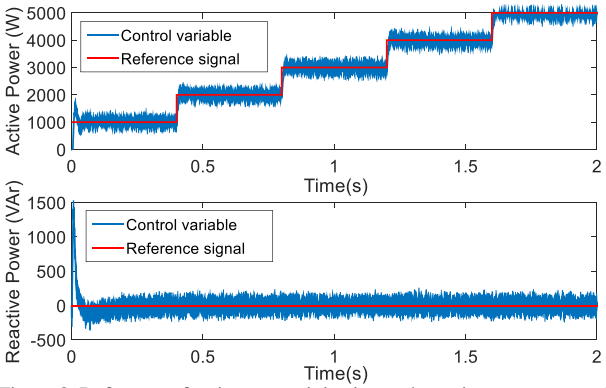

Figure 8. Reference of active power injection and reactive power control– test 1.

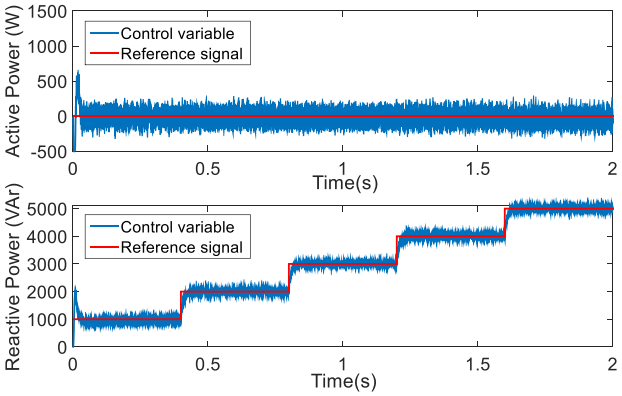

Figure 9. Reference of reactive power injection and active power control- test 2.

Using this active and reactive power profile, the inverter simulation was performed to measure the losses, considering all IGBTs and all diodes from each phase. The diode and IGBT losses can be seen in Fig. 10 and Fig. 11, respectively, during active power injection. As the current increases by the power injection, the losses also have their values higher. As can be seen, the diode has a greater increase during the switching process. The IGBTs, in its turn, has a greater increase during the conduction process.

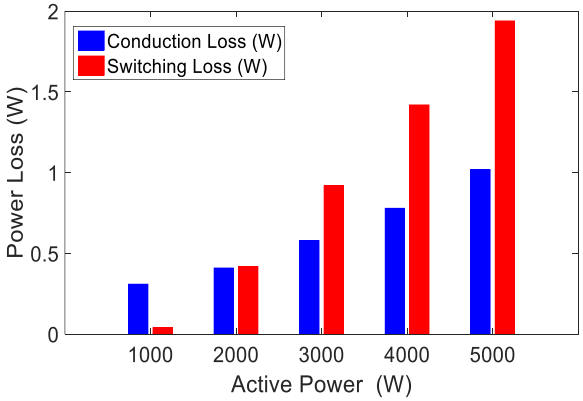

Figure 10. Power dissipation on Diode from phase 1 during active power injection.

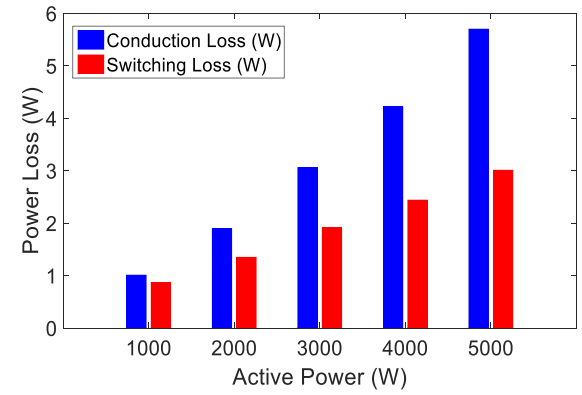

Figure 11. Power dissipation on IGBT from phase 1 during active power injection.

Also, it can be noticed that the losses in diodes are less than in IGBT. It happens because during the active power injection the diodes are less used.

PV inverter losses during reactive power injection are shown in Fig. 12 and Fig. 13, for diodes and IGBTs, respectively. It is possible to observe an increase in the diodes conduction losses during reactive power injection. On the other hand, a reduction in IGBTs switching and conduction losses is observed during reactive power injection. In this case, the loss distribution is more homogeneous because both diode and IGBT are equally used.

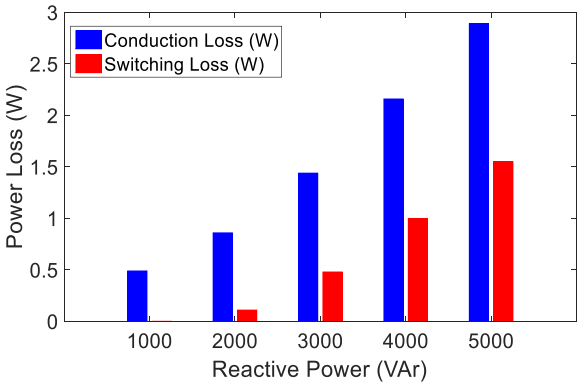

Figure 12. Power dissipation on Diode phase 1 during reactive power injection.

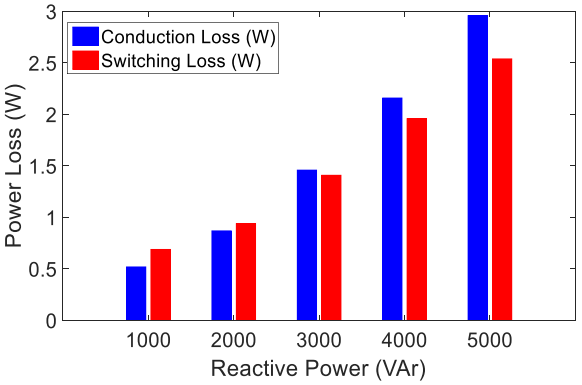

Figure 13. Power dissipation on IGBT phase 1 during reactive power injection.

Tables II and III show the total losses in the inverter. The losses shown in Table II are from four sources: IGBT losses, diode losses, passive damping (R_d) losses and dc-link capacitance (C_{bus}) losses. The total losses for IGBTs and diodes follow the same behavior seen for a single electronic component.

TABLE II. TOTAL LOSSES IN THE INVERTER (ACTIVE POWER)

Injected Power (kW)	Losses (W)				
	IGBT	Diode	R_d	C_{bus}	Total
1	11.23	2.25	4.51	0.53	13.56
2	19.64	5.06	4.51	1.03	24.77
3	29.48	8.98	4.51	1.85	38.50
4	40.26	13.18	4.51	2.99	53.48
5	52.09	17.90	4.51	4.46	69.94

TABLE III. TOTAL LOSSES IN THE INVERTER (REACTIVE POWER)

Injected Power (kVAr)	Losses (W)				
	IGBT	Diode	R_d	C_{bus}	Total
1	7.14	2.91	4.61	0.38	10.04
2	10.85	5.77	4.61	0.65	16.62
3	17.19	11.24	4.61	1.15	28.43
4	24.70	18.52	4.61	1.94	43.23
5	32.74	26.75	4.61	2.98	59.49

The R_d loss is not affected by the power injection increasing, because in this component only circulate high-order frequency current components. Active and reactive power are represented by currents in 60 Hz, thus, during increase in the active or reactive power injection, the inverter keeps similar harmonic current distortion impact, and its filters passive elements are not absolving additional harmonic content.

The C_{bus} losses are lower than all the other losses in the inverter. As can be seen in Table II and IV, its values increase by increasing the active power injection. Nevertheless, the C_{bus} loss represents about 9% of the total loss for a 5kW inverter. Based on the result, it could be concluded that the highest losses source are in the IGBTs followed by the diodes.

A further evaluation was conducted to analyze the IGBTs and diodes losses individually. The IGBT and diode losses are divided into switching and conduction losses in order to observe what is the main source of losses. As can be seen in Table IV, the greater losses come from the conduction for both IGBT and diodes. It happens because the used switching frequency is 6 kHz that is not a high frequency for semiconductor devices.

For reactive power injection, when the PV inverter is injecting 1kVAr, the switching losses are greater than conduction losses in the IGBT. Nevertheless, from 2kVAr,the conduction losses are greater. The power dissipation on diodes is always greater during the conduction.

The diode losses during reactive power injection (Table V) is greater than the diode losses for the active power injection (Table IV); the loss increases almost 50%. Thus, it is possible to conclude that adding reactive power in a PV inverter

decreases the inverter efficiency, besides, increase the stress in the diodes

TABLE IV. IGBT AND DIODE LOSSES IN THE INVERTER (ACTIVE POWER)

Power (kW)	IGBT Losses			Diode Losses		
	Total	Cond.	Switch.	Total	Cond.	Switch.
1	11.23	6.12	5.12	2.25	1.96	0.36
2	19.64	11.43	8.20	5.06	2.51	2.62
3	29.48	18.12	11.35	8.98	3.52	5.51
4	40.26	25.68	14.58	13.18	4.71	8.51
5	52.09	34.06	18.03	17.90	6.07	11.78

TABLE V. CONDUCTION AND SWITCHING LOSS (REACTIVE POWER)

Power (kVAr)	IGBT Losses			Diode Losses		
	Total	Cond.	Switch.	Total	Cond.	Switch.
1	7.14	2.95	4.18	2.91	2.90	0.01
2	10.85	5.21	5.64	5.77	5.08	0.69
3	17.19	8.71	8.48	11.24	8.46	2.78
4	24.70	12.86	11.84	18.52	12.62	5.90
5	32.74	17.53	15.21	26.75	17.45	9.30

In the last simulation, the active and reactive power were applied together. The power dissipation on the diode and the IGBT are showed in Fig.14 and Fig.15, respectively. As can be noticed, the power losses increase when the injection of active power increases.

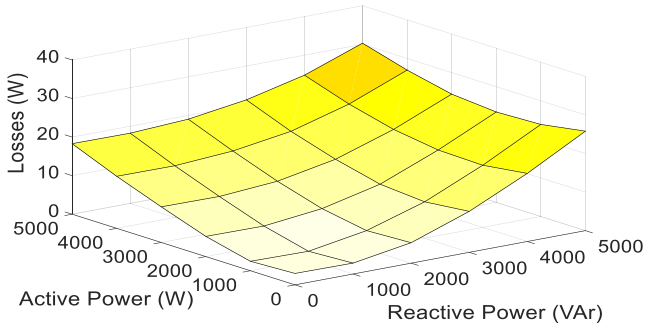

Figure 14. Surface of power dissipation on diode during active and reactive power injection.

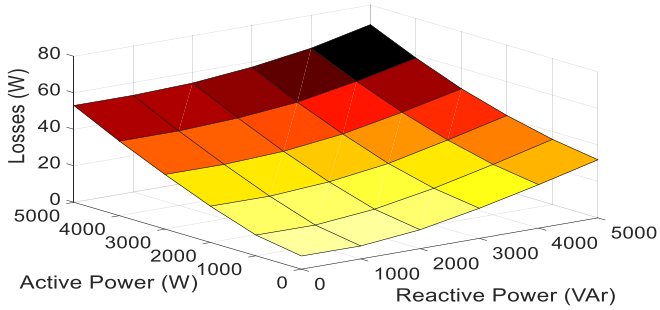

Figure 15. Surface of power dissipation on IGBT during active and reactive power injection.

In addition, the schematic thermal Foster model was used to estimate the temperature variation on the IGBTs and diodes. The results can be verified in Fig. 16 and 17. There is a greater variation in the diode temperature when the PV inverter is injecting reactive power. The same is not true for the IGBTs. In other words, the reactive power injection does not rise the temperature on this device as much as on diodes.

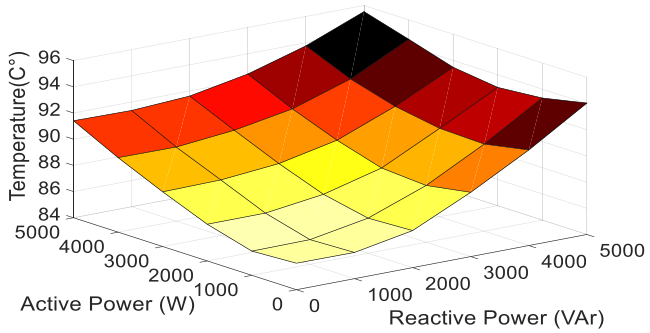

Figure 16. Average temperature for the diode for active and reactive power.

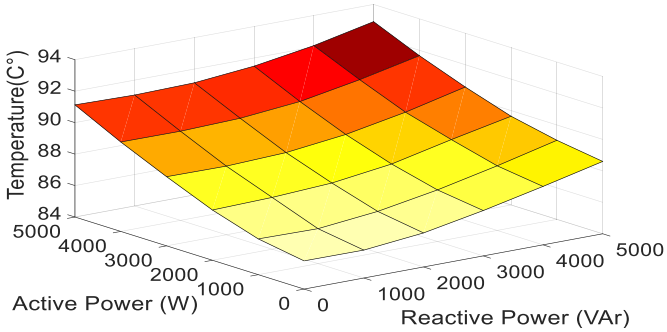

Figure 17. Average temperature for the IGBT for active and reactive power.

Based on the presented analysis, it can be concluded that the diode is the most affected component during reactive power injection. It reaches high levels of temperature. Although, both diode and IGBT are impacted during the reactive power injection, and it can cause a reduction in their reliability. The high temperature values can cause some damages on these devices. Thus, the entire PV inverter lifetime can be affected.

In addition, the schematic thermal Foster model was used to simulate the temperature variation on the IGBTs and Diodes on steady state. The results can be verified in Figure 18 for the worse case, when the PV inverter is injecting 5k of active power and 5k of reactive power.

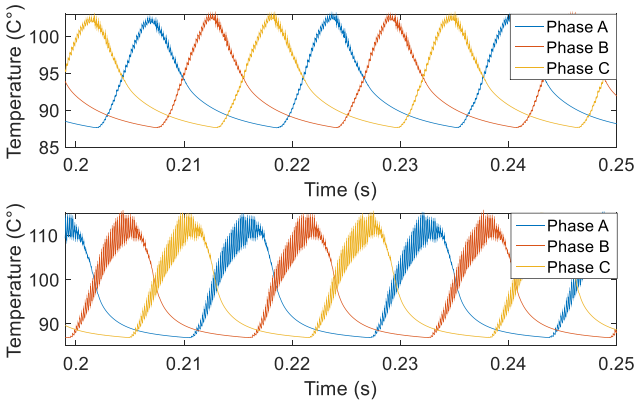

Figure 18. Temperature variation on the IGBT (top) and Diode (bottom) in steady state, worse case (5k of active power injecting and 5k of reactive power injecting).

CONCLUSION

This paper analyzes the power losses in the components of a PV inverter, during active and reactive power injections. Thermal performances of a 5kW PV inverter during active and reactive power shows that the total losses are similar for both situation. While the loss for active power represents 1.4%, the loss for reactive power is 1.2%, in nominal power conditions.

The electrical and thermal stresses of the devices are inversely related to the lifetime of the components. With the overused of the device, the lifetime tends to decrease. This fact can cause serious reliability and economic issues in PV inverter. Regulations may be made regarding limiting the reactive power injection by the PV inverter to the utility grid once the highest temperatures were found for this type of power.

The future work includes similar analysis of different inverter topologies and ratings. These results will enable to quantify reliability issues of the PV inverters and to perform cost-benefit analysis of how to adjust reactive power injection to supply voltage control in the distribution systems.

REFERENCES

[1] G. Masson e S. Orlandi, "Global Market Outlook for Solar Power," [Online]. Available: http://helapco.gr/pdf/Global_Market_Outlook_2015_-2019_lr_v23.pdf. [Acesso em 17 June 2016].

[2] R. M. Domingos, L. S. Xavier, A. F. Cupertino e H. A. Pereira, "Current control strategy for reactive and harmonic compensation with dynamic saturation," em *24th International Symposium on Industrial Electronics*, 2015.

[3] S. Ozdemir, S. Bayhan, I. Sefa e N. Altin, "Three-phase multilevel grid interactive inverter for PV systems with reactive power support capability," em *2015 First Workshop on Smart Grid and Renewable Energy*, 2015, pp. 1-6.

[4] R. K. Varma, B. Das, I. Axente e T. Vanderheide, "Optimal 24-hr utilization of a PV solar system as STATCOM (PV-STATCOM) in a distribution network," em *IEEE Power and Energy Society General Meeting*, 2011.

[5] A. Anurag, Y. Yang e F. Blaabjerg, "Thermal Performance and Reliability Analysis of Single-Phase PV Inverters With Reactive Power Injection Outside Feed-In Operating Hours," *IEEE Journal of Emerging and Selected Topics in Power Electronics,* vol. 3, pp. 870-880, 2015.

[6] I. Ndiaye, X. Wu e M. Agamy, "Impact of micro-inverter reactive power support capability in high penetration residential PV networks," em *IEEE 42nd Photovoltaic Specialist Conference*, 2015, pp. 1-6.

[7] S. M. Sreechithra, P. Jirutitijaroen e A. K. Rathore, "Impacts of reactive power injections on thermal performances of PV inverters," em *39th Annual Conference of the IEEE Industrial Electronics Society*, 2013.

[8] C. H. a. P. M. a. G. F. a. R. Ness, "IGBT and diode loss measurements in pulsed power operating conditions," em *Power Modulator Symposium*, 2004.

[9] X. H. a. S. L. a. S. S. a. W. Lian, "A Foster Network Thermal Model for HEV/EV Batterry Modeling," *IEEE Transactions on Industry Applications,* vol. 47, pp. 1692-1699, 2011.

[10] A. Wintrich, "IGBT4 and free wheeling diode CAL4 in IGBT," em *Appl. Note AN-9001,Germany* , 2009, pp. 1-12.

[11] A. Cagnano, E. D. Tuglie, M. Liserre e R. A. Mastromauro, "Online Optimal Reactive Power Control Strategy of PV Inverters," *IEEE Transactions on Industrial Electronics,* vol. 58, p. 10, 2011.